Saudi Pharmaceutical Journal 28 (2020) 1383–1391

Contents lists available at ScienceDirect

Saudi Pharmaceutical Journal

journal homepage: www.sciencedirect.com

Original article

Siphonocholin isolated from red sea sponge *Siphonochalina siphonella* attenuates quorum sensing controlled virulence and biofilm formation

Perwez Alam [a,*], Ali S. Alqahtani [a,*,1], Fohad Mabood Husain [b], Md. Tabish Rehman [a], Mohamed F. Alajmi [a], Omar M. Noman [a], Ali A. El Gamal [a], Shaza M. Al-Massarani [a], Mohammad Shavez Khan [c]

[a] Department of Pharmacognosy, College of Pharmacy, King Saud University, Riyadh, Saudi Arabia
[b] Department of Food Science and Nutrition, College of Food and Agriculture Sciences, King Saud University, Riyadh, Saudi Arabia
[c] National Bureau of Agriculturally Important Microorganisms, Maunath Bhanjan, India

ARTICLE INFO

Article history:
Received 30 May 2020
Accepted 7 September 2020
Available online 12 September 2020

Keywords:
Siphonochalina siphonella
Siphonocholin
Red sea sponge
Antipathogenic Quorum sensing
Biofilm
Molecular docking and simulation

ABSTRACT

Increasing incidence of multi-drug resistant bacterial pathogens, especially in clinical settings, has been developed into a grave health situation. The drug resistance problem demands the necessity for alternative unique therapeutic policies. One such tactic is targeting the quorum sensing (QS) controlled virulence and biofilm production. In this study, we evaluated a marine steroid Siphonocholin (Syph-1) isolated from *Siphonochalina* siphonella against *Chromobacterium violaceum* (CV) 12472, *Pseudomonas aeruginosa* (PAO1), Methicillin-resistant *Staphylococcus aureus* (MRSA) and *Acinetobacter baumannii* (BAA) for biofilm and pellicle formation inhibition, and anti-QS property. MIC of Syph-1 against MRSA, CV, PAO1 was found as 64 μg/mL and 256 μg/mL against BAA. At selected sub-MICs, Syph-1 significantly ($P \leq 0.05$) decreased the production of QS regulated virulence functions of CV12472 (violacein) and PAO1 [elastase, total protease, pyocyanin, chitinase, exopolysaccharides, and swarming motility]. The Syph-1 significantly decreased ($p = 0.005$) biofilm formation ability of tested bacterial pathogens, at sub-MIC level (PAO1 > MRSA > CV > BAA) and pellicle formation in A. baumannii (at 128 μg/mL). Molecular docking and simulation results indicated that Siph-1 was bound at the active site of BfmR N-terminal domain with high affinity. This study highlights the anti-QS and anti-biofilm activity of Syph-1 against bacterial pathogens reflecting its broad spectrum anti-infective potential.

1. Introduction

Infectious diseases are the most critical problem related to health and are the cause of increased morbidity and mortality among the human population (Ahmad et al., 2000). The bacterial infection is considered one of the most serious global health issues in the 21st century (Morris & Masterton, 2002). Bacteria have evolved to evade the action of antibiotics, leading to the rise and emergence of multiple drug-resistant bacterial strains. With increasing resistance of pathogens to antibiotics, there is a public health priority for exploring and developing alternative and effective anti-infective agents (Thanigaivel et al., 2015). Targeting virulence factors production and biofilm-forming ability of pathogens is one of the most promising and comparatively safer alternatives that has been under recent scientific attention (Husain et al., 2017). The majority of virulence genes, including those involved in various steps of biofilm formation, are under the control of quorum sensing (QS) networks in bacteria. Thus, targeting QS networking pathways in the bacteria has been focused on the development of novel anti-infective agents. There is growing interest in finding natural products/lead compounds capable of either blocking or modulating QS signaling pathways in bacteria (Husain et al., 2018).

Natural products from marine plants represent a wide variety of secondary metabolites which are used either directly as precursors or as lead compounds in the pharmaceutical industry (Shokeen et al., 2009). Many naturally occurring compounds obtained from marine plants have been studied and found to be effective in their

* Corresponding authors.
E-mail addresses: aperwez@ksu.edu.sa (P. Alam), alalqahtani@ksu.edu.sa (A.S. Alqahtani), onoman@ksu.edu.sa (O.M. Noman), salmassarani@ksu.edu.sa (S.M. Al-Massarani), shavezamu@gmail.com (M. Shavez Khan).
[1] Author to be considered as co-first author.
Peer review under responsibility of King Saud University.

Production and hosting by Elsevier

https://doi.org/10.1016/j.jsps.2020.09.002
1319-0164/

potential role as antimicrobial agents against pathogenic microorganisms (Cowan, 1999; Juneja et al., 2012). These compounds may inhibit bacteria through different mechanisms than the conventional antibiotics and therefore be of clinical value in the treatment of microbial infections (Saad et al., 2012). Several biologically active compounds with varying degrees of action, such as antitumor, anticancer, antimicrotubule, antiproliferative, cytotoxic, photoprotective, as well as antibiotic and antifouling properties, have so far been isolated from marine sources. Among marine organisms, the sponges (*Phylum Porifera*) continue to be a rich source of novel secondary metabolites with diverse and unique biological activities. They are even considered to be the more prolific producers of new marine natural products (Bergmann & Feeney, 1951; Villa & Gerwick, 2010; Mayer et al., 2011; Blunt et al., 2011). Until now, more than 5000 different compounds have been isolated from about 500 species of sponges (Müller et al., 2004). Species of the red sea sponge belonging to genus *Siphonochalina* are distributed throughout the Gulfs of Aqaba and Suez. *Siphonochalina siphonella*, a grey colonial tube-like sponge, is one of the few sponges known to produce squalene-derived cyclic ether triterpenes (Kashman et al., 2001). So far, about thirty compounds belonging to four different skeletal, namely, the sipholanes (Carmely & Kashman, 1983), siphonellanes (Carmely et al., 1983), neviotanes (Carmely & Kashman, 1986) and dahabanes (Kashman et al., 2001) have been reported from *S. siphonella* along with marine steroid Siphonocholin (ergosta-5-ene-3-ol; Siph-1; Fig. 1). However, little efforts have been made to evaluate the anti-infective potential of these compounds. The basic structure of the present study to search for a potential non-antibiotics theurapetic agents which interefere with secreation of numerous QS regulated virulence factors in pathogenic bacteria. Thus, this study was planned to evaluate the quorum-sensing controlled virulence and biofilm production attenuation property of Siph-1 against the *Chromobacterium violaceum* (CV) 12472 strain, *Pseudomonas aeruginosa* (PAO1), MRSA and *Acinetobacter baumannii* (BAA). An attempt has also been made to predict the mode of action of the compound using *in silico* molecular modelling.

2. Materials and methods

2.1. Bacterial strains

The bacterial strains under study were *Pseudomonas aeruginosa* (PAO1), *Chromobacterium violaceum* ATCC 12472, Methicillin-resistant *Staphylococcus aureus* ATCC 43,300 (MRSA) and *Acinetobacter baumannii* ATCC BAA747 (BAA). All strains were maintained on the Luria Bertani (LB) broth solidified with 1.5% agar (Oxoid).

2.2. Isolation of Siphonocholin (Siph-1) from S. siphonella

The marine sponge (*S. siphonella*; 95g) was collected from Sharm Obhur (Jeddah, Saudi Arabian red sea coast), freeze-dried, and macerated using ethanol (70%) at room temperature. The obtained extract was filtered, and the solvent was evaporated under reduced pressure using rotavapour at 40 °C. The dried ethanol extract (30 g) was then suspended in water and partitioned (successively) with n-hexane, dichloromethane, and n-butanol to collect the corresponding extracts. All the extracts (n-hexane, dichloromethane, and n-butanol) were merged based on their close similarity on TLC. The combined extracts were purified by applying it on the top of a silica gel packed column (Merck) and eluted with n- hexane. The mobile phase polarity was progressively increased with ethyl acetate and with 25% ethyl acetate and direct crystallization of the obtained fraction afforded compound Syph-1 (125 mg). The structure was established by using

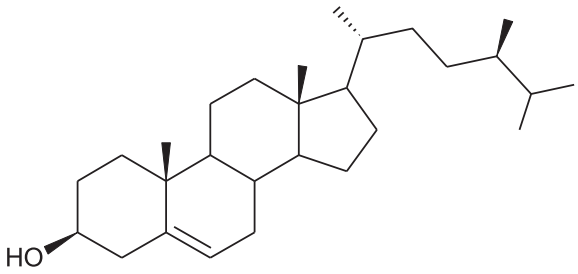

Fig. 1. Chemical structure of Siph-1.

1D-NMR, 2D-NMR, IR, HREIMS, and compared with the result published by Ge et al., 2010. The compound was reconstituted in DMSO, and final concentration experimental mixture was maintained at 0.1% of DMSO.

2.3. Determination of minimum inhibitory concentration (MIC) of Syph-1

The MIC of Syph-1 against all the bacterial pathogens was determined by using the CLSI microbroth dilution method (Al-Shabib et al., 2016). Concentrations below the MICs were considered sub-inhibitory and were further used to study the anti-QS and biofilm inhibitory properties. Growth of tested bacteria was also evaluated at different concentration of Syph-1 by observing the OD at 600 nm.

2.4. Screening of syph-1 for quorum sensing inhibition

Biosensor strain *C. violaceum* (CV)12472 was inoculated to in Erlenmeyer flasks containing Luria broth (LB) and the test agent. The flasks were incubated at 27 °C with 150 rev/min agitation for 24 h in a shaking incubator. Violacein production by CV12472 in the presence and absence of Syph-1 was studied using the method described by (Husain, 2015a). Azithromycin was used as positive control (Data not shown).

2.5. Effect on sub-MIC of Syph-1 on QS-regulated virulence

Effect of Sub-MICs of Syph-1 on virulence factors of *P. aeruginosa* PAO1 such as LasB elastase, protease, pyocyanin, chitinase, EPS production, and quantification was determined using protocols described previously (Al-Shabib et al., 2016). Swarming motility was determined as described earlier (Husain & Ahmad, 2013). Briefly, an overnight culture of test pathogen was point inoculated at the center of the LB medium consisting of 0.5% agar with or without various sub-inhibitory concentrations of the test compound. Additionally, Azithromycin was used as positive control (Data not shown).

2.6. Assessment of pellicle formation

Pellicle formation in *A. baumanii* and *P. aeruginosa* was assayed using the method described by Marti et al. 2011. Treated and untreated bacteria were incubated for 72 h at 25 °C and 35 °C. The amount of pellicle was determined by removing the pellicle and suspending it in phosphate buffer saline. OD was taken at 600 nm. The results presented are the averages of at least three experiments performed independently.

2.7. Biofilm inhibition assay

The effect of Syph-1 on biofilm formation was measured using the polyvinyl chloride biofilm formation assay (O'Toole & Kolter, 1998).

Briefly, overnight cultures of test pathogens were re-suspended in fresh LB medium in the presence and absence of the test compound and incubated at 30 °C for 24 h. The biofilms were stained with a crystal violet solution and quantified by solubilizing the dye in ethanol and measuring the absorbance at OD_{470}. For biofilm inhibitory activity also we have also incorporated Azithromycin as positive control (Data not shown).

2.8. Molecular docking and molecular dynamics simulation

Molecular docking of Siph-1 with proteins involved in the virulence of different pathogens was performed using different modules of Schrodinger suite-2018 (Schrodinger, LLC, NY, USA) as described earlier (Rehman et al., 2019; Rehman et al., 2014). The structure of ligand (Siph-1) was drawn on 2D sketcher, and a maximum of 32 conformations of Siph-1 were generated pH 7.0 ± 2.0 using Epik (Schrodinger, LLC, NY, USA). The energies of all the possible conformations of Siph-1 were minimized using OPLS3e forcefield. The X-ray crystal structures of LasR (Pdb Id: 3IX4), Vfr (Pdb Id: 2OZ6), PqsA (Pdb Id: 5OE3), QscR (Pdb Id: 3SZT) and BfmR (Pdb Id: 6BR7) were downloaded from RCSB database. Prior to molecular docking structures of proteins were optimized by removing any non-essential heterogeneous molecule, including crystal water molecules, optimizing hydrogen bonding network by adding hydrogen atoms and minimizing the complete structure using OPLS3e forcefield. Grid maps were generated by selecting the centroid of the ligand-bound (if any) in the X-ray structure of the respective protein or using the SiteMap (Schrodinger, LLC, NY, USA) to generate the most probable binding site. The dimensions of grid box for LasR, Vfr, PqsA, QscR, and BfmR were 72 × 72 × 72 Å, 64 × 64 × 64 Å, 64 × 64 × 64 Å, 72 × 72 × 72 Å, and 80 × 80 × 80 Å respectively. Glide (Schrodinger, LLC, NY, USA) was used to perform molecular docking between Siph-1 and different virulence proteins. The docking affinity (K_d) of Siph-1 towards various virulence proteins was calculated using the following relation, as described previously (Rehman et al., 2016).

$$\Delta G = -RT\ln K_d$$

where R and T were Boltzmann's constant (=1.987 cal mol^{-1} K^{-1}) and temperature (=298 K), respectively.

The stability of protein–ligand interaction was accessed by performing molecular dynamics simulation using Desmond (Schrodinger, LLC, NY, USA). The simulation was performed in an orthorhombic box for 25 ns at 298 K and 1 atm pressure using NPT assemble. Boundaries of the simulation box were at least 10 Å away from the protein–ligand complex. TIP3P water model was employed to solvate the system, and proper counter-ions were added to neutralize the system. The physiological conditions were mimicked by adding 150 mM NaCl. The temperature and pressure were maintained using Nose-Hoover Chain thermostat and Martyna-Tobias-Klein barostat, respectively. All the trajectories were analyzed, and final figures were prepared in Maestro (Schrodinger, LLC, NY, USA).

2.9. Statistical analysis

All experiments were performed in triplicates, and the data obtained from experiments were presented as mean values, and the difference between control and test were analyzed using student's *t*-test.

3. Results and discussion

3.1. Determination of MIC

Minimum inhibitory concentration (MIC) was determined for the Syph-1 against the test microorganisms viz. MRSA, *C. violaceum* (CV12472), *P. aeruginosa* (PAO1), and *A. baumanii* (BAA) (Table 1). Additionally, growth kinetics of each bacterium has been evaluated under the effect of their respective sub-MICs. No significant decrease in growth of bacteria under the affect of selected concentration of Syph-1 was observed (Fig. 2).

3.2. Quorum sensing (QS) inhibition assay of Syph-1

In this study, Syph-1 was found to inhibit the production of violacein in CV12472 strain (wild type) in a dose-dependent manner without affecting the bacterial growth. It is clearly evident from Fig. 3(A) that the maximum reduction of violacein production (58%) was achieved at 32 μg/mL of Siph-1 while at lower concentrations 4, 8, and 16 μg/mL, the percentage reduction in violacein production was found as 8, 22 and 34%, respectively. The violacein inhibition under the effect of Syph-1 indicates the anti-QS potential of the isolated compounds. Violacein pigment production in *C. violaceum* is regulated by QS and coordinated by the CviIR-dependent QS system (Al-Shabib et al., 2016). Violacein inhibition assay is used extensively for the screening of potential anti-QS compounds (McClean et al., 1997). Similar inhibition of QS mediated production violacein in *C. violaceum* was reported with methanolic extracts of three marine sponges viz. *Aphrocallistes bocagei Haliclona megastoma* and *Clathria atrasanguinea* (Annapoorani et al., 2012).

3.3. Effect of Syph-1 on virulence factors of P. aeruginosa (PAO1)

A 4-quinolone dependent QS is integrated with AHL-dependent signaling by opportunistic human pathogen PAO1. Thus, the quorum-sensing systems (*las*, *rhl*, and *pqs*) of PAO1 control the production of numerous extracellular virulence factors (viz. elastase, the LasA protease, alkaline protease, swarming motility, exopolysaccharide, and pyocyanin) (Husain et al., 2018). The effect of syph-1(sub- MICs) on virulence factors of PAO1 is illustrated in Fig. 3B.

The sub-MICs of syph-1 showed significant ($p \leq 0.001$) reduction in elastase activity in the culture supernatant of PAO1. The maximum inhibition of elastase activity (76%) was found when PAO1 was cultured with 32 μg/mL of syph-1. Syph-1 demonstrated the percent inhibition of elastase in PAO1 in a dose-dependent manner (Fig. 3B). The elastase enzyme degrades the structural components of infected tissue that increase the intrusiveness and progression of the pathogen. The finding of this study is supported by the study published by Musthafa et al. (2017), which revealed the significant LasB activity inhibition by extracts of fruits as well as edible plants. Earlier research suggested that the medicinal plant extracts rich in flavonoids exert significant inhibition of QS dependent expression of elastase in PAO1. Recently the bark and seed extract of *Sclerocarya birrea* exhibited the significant inhibition of elastase activity (Sarkar et al., 2015).

Pyocyanin (a blue colored toxin regulated by QS) and phenazine-1-carboxylic acid (precursor of pyocyanin) cause apoptosis in neutrophils and damage the neutrophil-facilitated host defense (Fothergill et al., 2007). Syph-1 at sub-lethal concentrations displayed a substantial reduction in the production of pyocyanin. The maximum reduction in pyocyanin production (78%) was found when PAO1 was cultured with the highest tested sub-MIC (32 μg/mL) of syph-1, followed by 62, 52 and 22% at 16, 8,

Table 1
Minimum inhibitory concentration (MIC) of Siph-1 against bacterial pathogens.

Compound	MRSA (μg/mL)	*C. violaceum* (CV12472) (μg/mL)	*A. baumanii* (BAA) (μg/mL)	*P. aeruginosa* (PAO1) (μg/mL)
Siph-1	64	64	256	64

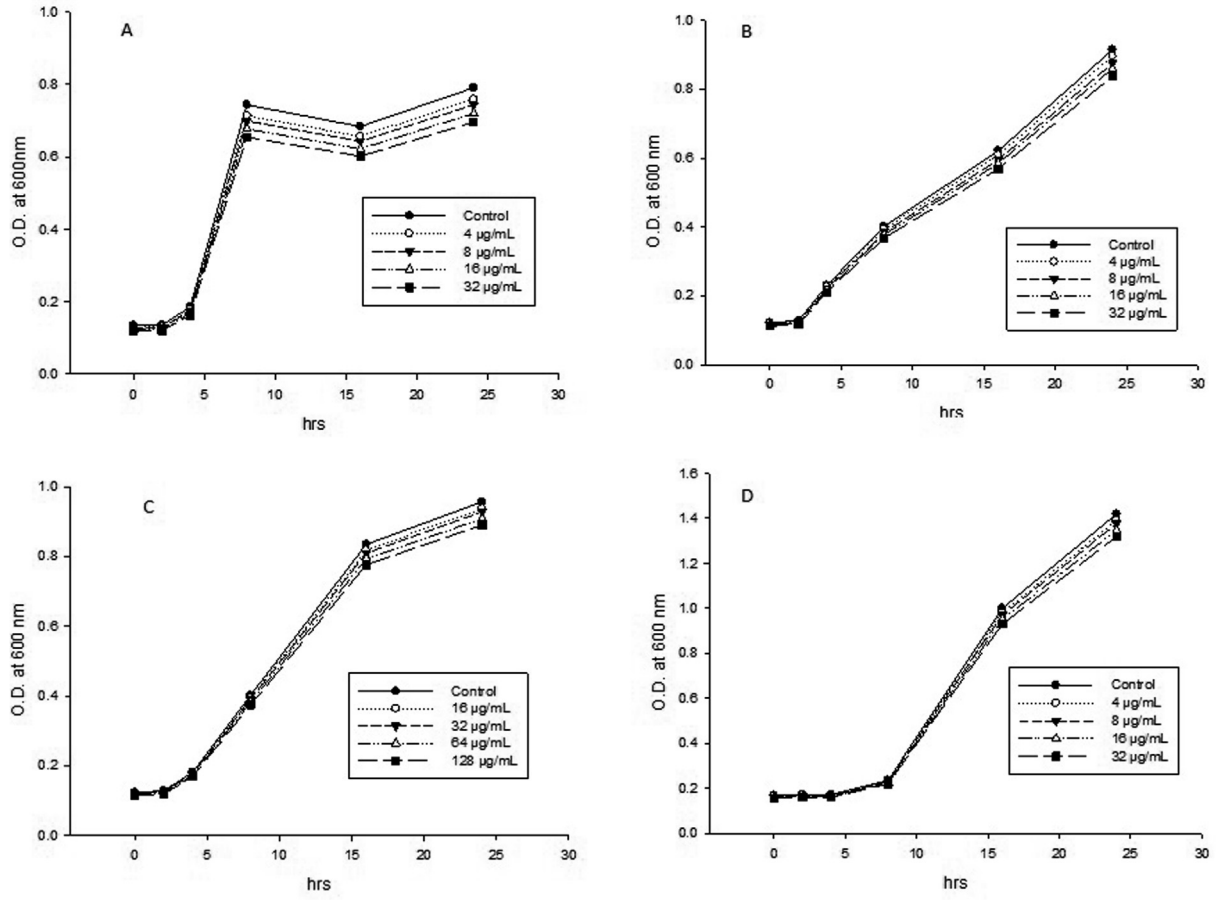

Fig. 2. Growth kinetics of A) PAO1, B) MRSA, C) BAA and D) CV12472 in the presence and absence of respective sub-MICs of Syph-1.

and 4 μg/mL, respectively (Fig. 3B). The recent research published demonstrated that the acetone and methanol extract of sponge *Ochridaspongia rotunda* reduced the production of pyocyanin by 42.4 and 49.9%, respectively (Pejin et al., 2014), which validated the current findings on pyocyanin reduction by syph-1.

It has been observed that on treatment with sub-MICs of the syph-1, there was a significant decrease (10–68%) in Chitinase activity in PAO1 (Fig. 3B) which was in accordance with the findings reported on *T. foenum-graceum* (21–48%) and *M. indica* (21–55%) (Husain et al., 2017).

Exopolysaccharide (EPS) production and swarming motility by pathogens play an important part in the initiation, maturation, and maintenance of the biofilm architecture (Hentzer & Givskov, 2003). Hence, any intervention in EPS production and motility by pathogens will certainly affect the formation of biofilm. In this experiment, the treatment of MRSA, PAO1, BAA, and CV with sub-MICs of Syph-1 exhibited a significant decrease in the production of EPS production to the level ranging from 20 to 42% (Fig. 3C). At 32 μg/mL of the compound, EPS production was maximally reduced in PAO1. Also, swarming motility of pathogens PAO1, BAA and CV were reduced significantly (10–18%) when treated with sub-MICs of syph-1 (Fig. 3D). This statistically significant decrease in the EPS and motility production is in accordance with the report published on *Trigonella foenum-graceum* seed extract (Husain et al., 2015b). Since EPS is integral part of biofilm matrix, it highly likely that compound/bioactive extracts interfering EPS production will be effective against biofilm forming ability of pathogenic bacteria (Rabin et al., 2015).

3.4. Assessment of pellicle formation

Pellicle formation was evaluated by using *A. baumannii* and *P. aeruginosa* in glass tubes containing LB broth at two different temperatures (25 °C and 35 °C). After a span of 24 h, the formation of a thin pellicle started on the media surface, and an opaque, robust, thick pellicle covered the whole media surface more at temperature 25 °C in comparison at 35 °C at the end of the third day. It revealed that the growth of pellicle occurred at 25 °C and this is in agreement with the report of Marti et al. 2011. The addition of Siph-1 (128 μg/mL) significantly decreased the pellicle formation in *A. baumanii* (Fig. 4A1). Similarly, at 32 μg/mL considerably reduced pellicle formation was observed in PAO1 (Fig. 4A2). *P. aeruginosa* and *A. baumannii* colonizes the upper surfaces of static liquids and form biofilms at air–liquid interfaces by a process called pellicle formation, which is a type of biofilm formation. This interface is important for aerobic bacteria as they obtain the

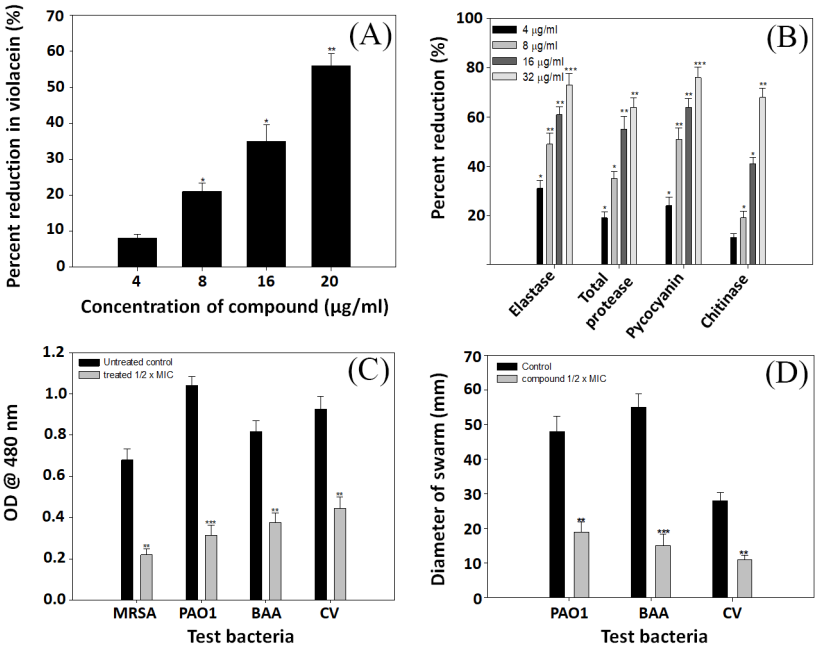

Fig. 3. (A) Quantitative assessment of percentage violacein inhibition in *C. violaceum* 12472 by sub-MICs of Siph-1. (B) Effect of sub-MICs of compound Siph-1 on virulence factor production in *P. aeruginosa*. (C) Effect of ½ x MICs of Siph-1 on the EPS production in the test pathogens. (D) Effect of ½ x MICs of compound Siph-1 on the swarming motility in the test pathogens. (All of the data are presented as mean ± standard deviation. *, $p \leq 0.05$; **, $p \leq 0.005$; ***, $p \leq 0.001$).

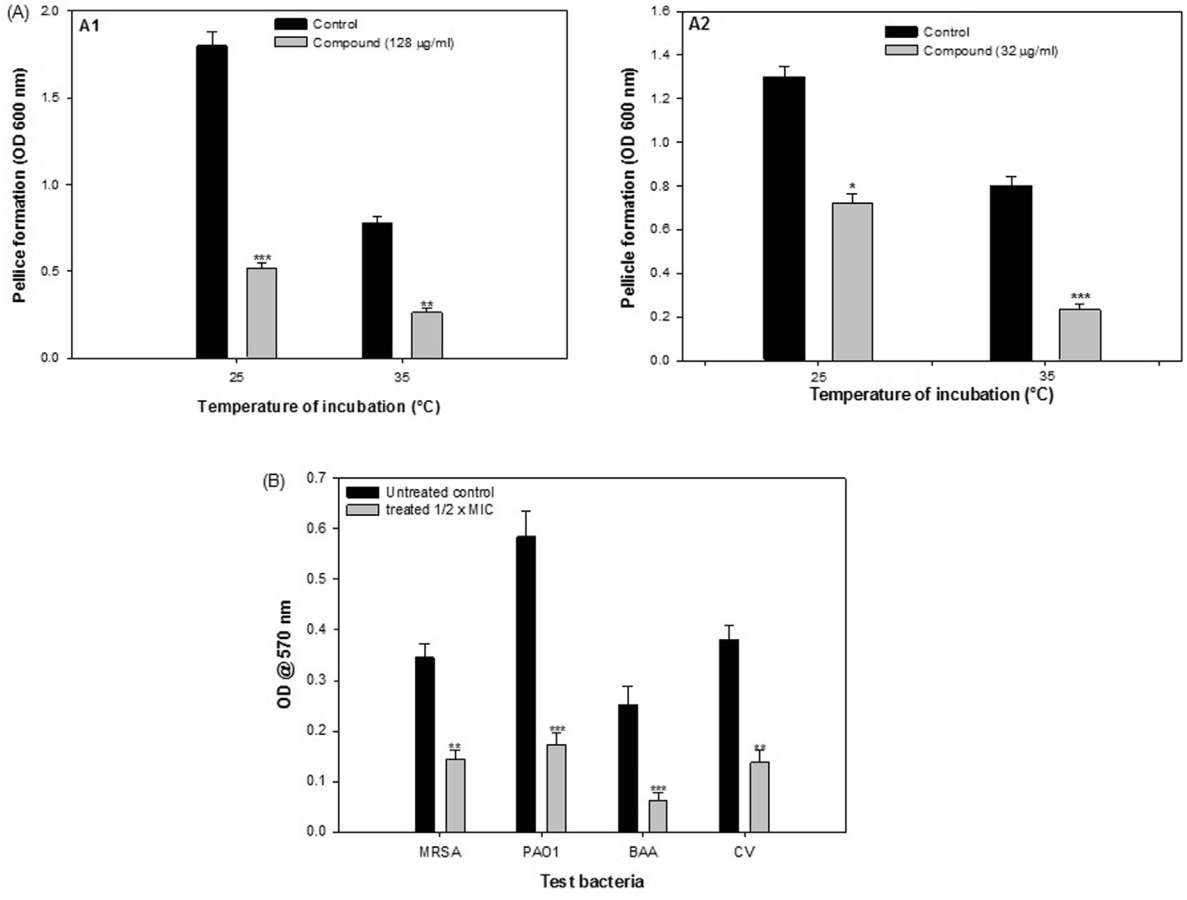

Fig. 4. (A) Effect of ½ x MIC of Siph-1 on the pellicle formation as determined by spectrophotometry at OD600. (B) Activity of ½ x MICs of Siph-1 against biofilms of selected pathogens using microtitre plate assay. (All of the data are presented as mean ± standard deviation. *, $p \leq 0.05$, **, $p \leq 0.005$, ***, $p \leq 0.001$).

Table 2
Molecular docking of Siph-1 with different virulent factors (LasR, PqsA, Vfr, QscR and BfmR).

Virulent factors	Docking energy, ΔG (kcal mol^{-1})		Docking affinity, Kd (M^{-1})	
	X-ray bound ligand/inhibitor	Siph-1	X-ray bound ligand/inhibitor	Siph-1
LasR	−12.32	NB	1.09×10^{9}	NB
PqsA	−13.64	−4.43	1.01×10^{10}	1.77×10^{3}
Vfr (site 1)	−10.94	−4.97	1.06×10^{8}	4.42×10^{3}
Vfr (site 2)	−7.31	−4.02	2.29×10^{5}	8.88×10^{2}
QscR	−7.30	−4.71	2.26×10^{5}	2.85×10^{3}
BfmR	NA	−7.21	NA	1.94×10^{5}

NB stands for no binding; NA stands for not available.

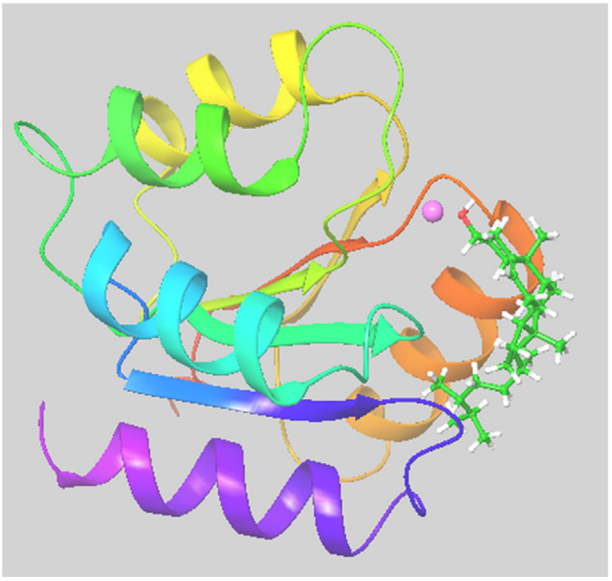

Fig. 5. Binding of Siph-1 at the active site of BfmR as revealed by molecular docking.

oxygen from the air and nutrients from the liquid media (Kentache et al., 2017). Our findings are in agreement with those reported for curcumin, it significantly reduced the pellicle formation in *A. baumanii* at 50 μg/mL (Raorane et al., 2019).

3.5. Biofilm inhibition assay

Biofilm is a complex accumulation of microorganisms and is the principal reason for *P. aeruginosa* pathogenesis (Caraher et al., 2007). Biofilms are the reason of severe insistent infection, and biofilm formation is considered as one of the potential drug targets to combat drug-resistant chronic infections (Wu et al., 2015). The Syph-1 exhibited a significant decrease in the biofilm formation ability of MRSA, PAO1, BAA, and CV at the sub-MIC level, and it was found in the order of PAO1 > MRSA > CV > BAA (Fig. 4B). Our findings on biofilm inhibition find support from the observations made with a sponge-inspired compound Dibromohemibastadin (Le Norcy et al., 2017). This compound reduced biofilm formation significantly in *Paracoccus* sp., *P. aeruginosa* PAO1, *Pseudoalteromonas* sp. and *Bacillus* sp.

3.6. Molecular docking and simulation analysis

Nature of the interaction between Siph-1 and virulence factors (LasR, Vfr, PqsA, QscR, and BfmR) and their stability was evaluated by performing molecular docking and molecular dynamics simulation, respectively. We first screened the binding affinity of Siph-1 towards different virulence factors by performing molecular docking in extra-precision (XP) mode (Table 2). We found a weak interaction of Siph-1 with PqsA, Vfr (site 1, and site 2), and QscR as their docking energies varied within −4.02 to −4.97 kcal mol^{-1}. Siph-1 showed relatively high docking energy (-7.21 kcal mol^{-1}) and hence docking affinity (1.94×10^{5} M^{-1}) towards BfmR. However, no interaction was observed in the molecular docking of Siph-1 with LasR.

In *A. baumanii*, BfmRS represents a two-component system involved in the formation of biofilms and virulence (Tomaras et al., 2008; Gaddy & Actis, 2009). BfmR is a master regulator of *A. baumanii csu* operon, controlling the expression of *csuC* and *csuE* genes. Primarily, these genes are responsible for the attachment of biofilms to abiotic surfaces. Moreover, BfmR controls pilin production and hence cell motility by regulating the chaperone-usher assembly system (*csuA/BABCDE*). The three-dimensional structure of BfmR constitutes two domains, the N-terminal receiver domain, and the C-terminal effector domain. The N-terminal domain contains a well-conserved site of phosphorylation/activation by histidine kinase, while the C-terminal domain contains a putative DNA-binding site (Russo et al., 2016; Draughn et al., 2018). Since the structural information of BfmR is incomplete due to non-availability of the X-ray crystal structure of C-terminal domain, we performed molecular docking only on the N-terminal domain.

An analysis of the interaction between Siph-1 and BfmR has revealed that Siph-1 was bound at the active site of BfmR located at the mouth of the central cavity near the N-terminal end (Fig. 5). Siph-1 was surrounded by Mg^{2+} ion, hydrophobic residues (Leu19, Met60, Leu84, Ala86, Pro108, Val109, and Pro111), polar residue (Thr23), charged residues (Glu14, Asp15, Asp16, Asp58, and Lys106) (Fig. 6A). In order to determine the stability of the Siph-1-BfmR complex, molecular dynamics simulation was performed for 25 ns. The interaction pattern observed after molecular dynamics simulation showed that the hydroxyl group of Siph-1 formed an interaction with Mg^{2+} and a hydrogen bond with Asp58 for 100% and 46% of simulation time, respectively (Fig. 6B). Moreover, Siph-1 was surrounded by hydrophobic residues (Leu19, Leu22, Met60, and Ala86) and charged residues (Glu14, Asp15, and Asp58). It is significant to note that Asp15, Asp58, and Met60 play a crucial role in maintaining the orientation of Mg^{2+} at the active site of BfmR (Draughn et al., 2018). Variation in root mean square deviation (RMSD) values gives an insight into the fluctuation of Cα-atoms and hence overall conformation of the protein structure. The RMSD values of BfmR alone or in complex with Siph-1 were observed to vary between 0.5 and 1.8 Å throughout the simulation, which is much lower than the acceptable limit of 2.0 Å (AlAjmi et al., 2018). After initial fluctuations, the RMSD values were estimated to plateau around 1.73 Å and 1.27 Å in the case of BfmR alone and BfmR-Siph-1 complex, respectively (Fig. 7A). Similarly, root mean square fluctuation (RMSF) gives an understanding of the variations in the fluctuations of individual amino acid residues throughout simulation time. It is evident from Fig. 7B that there was a huge fluctuation (4.5 and 3.0 Å) in the

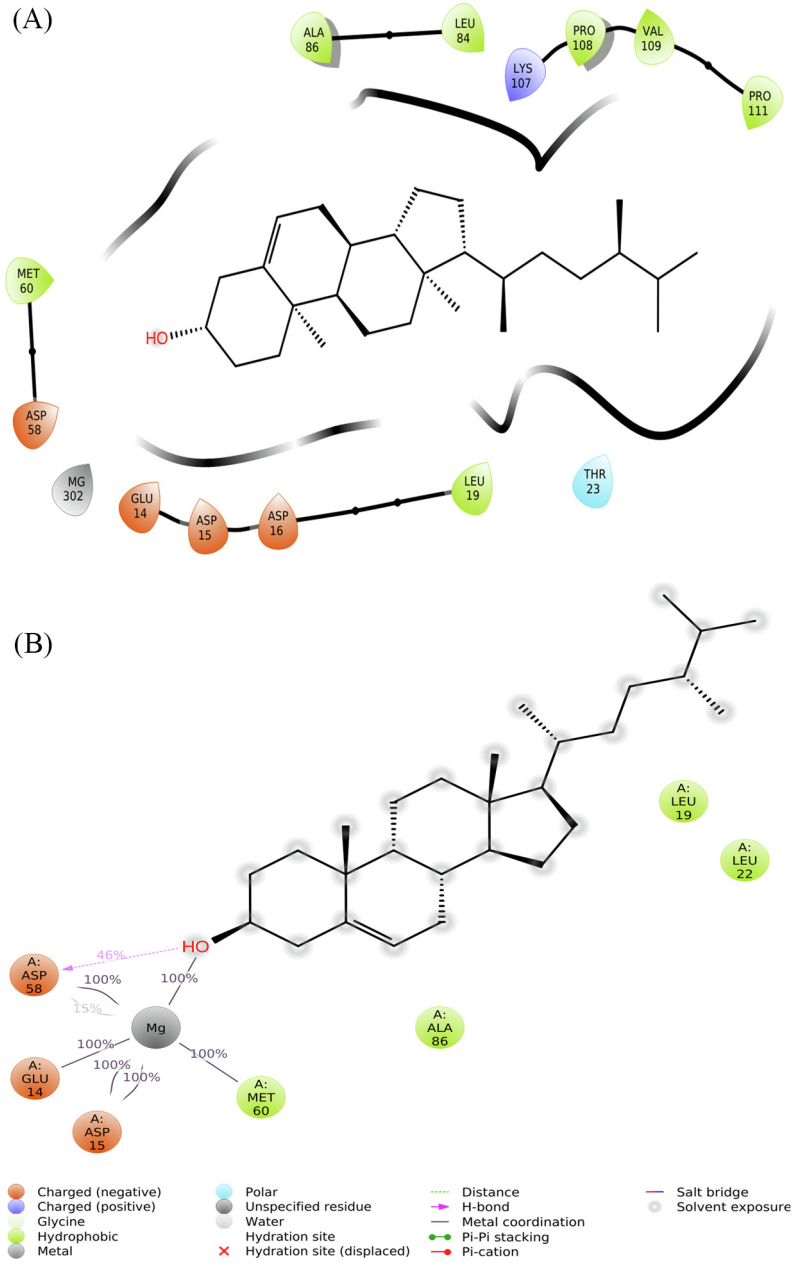

Fig. 6. Molecular docking of Siph-1 with BfmR (A) before, and (B) after molecular dynamics simulation.

amino acid residues located at the N-terminal as well as C-terminal ends, respectively. The RMSF values (Blue line) of residues located between the two ends varied with the acceptable limit, and they coincide with the experimentally determined X-ray B-factor (Red line). The vertical blue line represents the position of amino acid residues making contact with Siph-1. Further, the stability of Siph-1-BfmR complex was also indicated by a constant radius of gyration (rGyr) of around 4.5 Å throughout the simulation time (Fig. 7C). Similarly, the solvent-accessible surface area (SASA) of the Siph-1-BfmR complex did not change significantly over the simulation time, indicating a stable Siph-1-BfmR complex (Fig. 7D).

Earlier, the X-ray crystal structure of BfmR has shown that it harbors an active site comprising Glu14, Asp15, Asp16, Asp58, Thr85, Tyr104, and Lys107 (Russo et al., 2016). It is interesting to note that Asp58 of BfmR is a conserved residue that undergoes autophosphorylation to activate the receptor. The phosphorylation of Asp58 induces an equilibrium shift towards active conformation, which is a 2-fold symmetrical homodimer of α4-β5-α5 face (Bachhawat & Stock, 2007). The active homodimer then binds DNA and controls the transcription of downstream genes. In addition to homodimerization, activation of BfmR also involves a paradigm shift of Thr85 towards phosphorylated Asp58 in such a way that the hydroxyl of Thr85 forms a hydrogen bond with the phosphate group. This conformational change promotes Tyr104 on β5 strand to move its bulky chain away from the α4-β5-α5 dimerization interface into the volume previously occupied by Thr85 side chain. Thus, it has been proposed that any small molecule which interrupts BfmR dimerization and hence its activation would act as potential drug molecule (Russo et al., 2016). In this study, we proposed Siph-1 as a potential inhibitor of BfmR as it directly interacts with active side residues like Glu14, Asp15, Asp16, Asp58, and binds some other residues located at α4 strand like Leu84 and Ala86, and α5 strand such as Pro111.

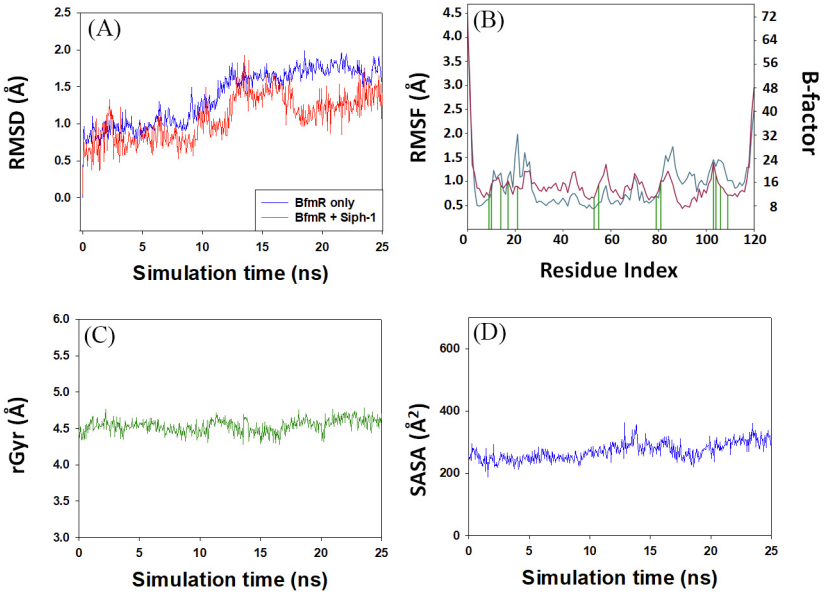

Fig. 7. Molecular dynamics simulation of Siph-1 with BfmR. (A) Variation in root mean square deviation (RMSD) values of BfmR alone or Siph-BfmR complex, and (B) root means square fluctuation (RMSF) values of Siph-1-BfmR complex, (C) variation in radius of gyration (rGyr) of Siph-1-BfmR complex, and (D) variation in solvent accessible surface area (SASA) of Siph-1-BfmR complex.

4. Conclusion

This study highlights the anti-infective potential of the Siph-1 by targeting the QS-controlled virulence and the biofilm production of pathogens. A detailed mechanism of action is delineated in this study using a computational approach. Molecular docking and molecular dynamics simulation showed that Siph-1 binds primarily to BfmR with high affinity, and the Ship-1-BfmR complex is stable. Further, detailed *in vivo* sand toxicological studies are required for the potential application of the Syph-1 as a therapeutic agent.

Declaration of Competing Interest

The authors report no declaration of interest. The authors alone are responsible for the content and writing of the paper.

Acknowledgement

The authors are grateful to the Researchers Supporting Project Number (RSP-2020/132), King Saud University, Riyadh, Kingdom of Saudi Arabia.

References

Ahmad, I., Mehmood, Z., Mohammad, F., Ahmad, S., 2000. Antimicrobial potency and synergistic activity of five traditionally used Indian medicinal plants. J. Med. Aromat. Plants. 22 (4), 173–176.

AlAjmi, M.F., Rehman, M.T., Hussain, A., Rather, G.M., 2018. Pharmacoinformatics approach for the identification of Polo-like kinase-1 inhibitors from natural sources as anti-cancer agents. Int. J. Biol. Macromol. 116, 173–181.

Al-Shabib, N.A., Husain, F.M., Ahmed, F., Khan ,R.A. et al., 2017. Biogenic synthesis of Zinc oxide nanostructures from Nigella sativa seed: Prospective role as food packaging material inhibiting broad-spectrum quorum sensing and biofilm. Sci Rep. 2016, 6, 36761. Erratum in: Sci Rep. 7, 42266.

Annapoorani, A., Jabbar, A.K.K.A., Musthafa, S.K.S., Pandian, S.K., Ravi, A.V., 2012. Inhibition of quorum sensing mediated virulence factors production in urinary pathogen *Serratia marcescens* PS1 by marine sponges. Indian J. Microbiol. 52, 160–166.

Bachhawat, P., Stock, A.M., 2007. Crystal structures of the receiver domain of the response regulator PhoP from *Escherichia coli* in the absence and presence of the phosphoryl analog beryllofluoride. J. Bacteriol. 189 (16), 5987–5995.

Bergmann, W., Feeney, R.J., 1951. Contributions to the study of marine products. XXXII. The nucleosides of sponges. I. J Org Chem. 16 (6), 981–987.

Blunt, J.W., Copp, B.R., Munro, M.H., Northcote, P.T., Prinsep, M.R., 2011. Marine natural products. Nat Prod Rep. 28 (2), 196–268.

Caraher, E., Duff, C., Mullen, T., McKeon, S., Murphy, P., Callaghan, M., McClean, S., 2007. Invasion and biofilm formation of *Burkholderia dolosa* is comparable with *Burkholderia cenocepacia* and *Burkholderia multivorans*. J. Cyst. Fibros. 6 (1), 49–56.

Carmely, S., Kashman, Y., 1983. The sipholanes, a novel group of triterpenes from the marine sponge *Siphonochalina siphonella*. J. Org. Chem. 48 (20), 3517–3525.

Carmely, S., Kashman, Y., 1986. Neviotine-A, a new triterpene from the Red Sea sponge *Siphonochalina siphonella*. J. Org. Chem. 51 (6), 784–788.

Carmely, S., Loya, Y., Kashman, Y., 1983. Siphenellinol, a new triterpene from the marine sponge *Siphonochalina siphonella*. Tetrahedron. Lett. 24 (34), 3673–3676.

Cowan, M.M., 1999. Plant products as antimicrobial agents. Clin. Microbiol. Rev. 12 (4), 564–582.

Draughn, G.L., Milton, M.E., Feldmann, E.A., Bobay, B.G., Roth, B.M., Olson, A.L., Thompson, R.J., Actis, L.A., Davies, C., Cavanagh, J., 2018. The structure of the biofilm-controlling response regulator BfmR from *Acinetobacter baumannii* reveals details of Its DNA-binding mechanism. J. Mol. Biol. 430, 806–821.

Fothergill, J.L., Panagea, S., Hart, C.A., Walshaw, M.J., Pitt, T.L., Winstanley, C., 2007. Widespread pyocyanin overproduction among isolates of a cystic fibrosis epidemic strain. BMC Microbiol. 7, 45.

Gaddy, J.A., Actis, L.A., 2009. Actis, regulation of *Acinetobacter baumannii* biofilm formation. Fut. Microbiol. 4, 273–278.

Ge, J.H., Gao, C.H., Wang, P., Wen, L.J., Qi, S.H., 2010. Study on the Chemical Constituents of *Antipathes dichotoma*. Zhong Yao Cai. 33 (9), 1403–1405.

Hentzer, M., Givskov, M., 2003. Pharmacological inhibition of quorum sensing for the treatment of chronic bacterial infections. J. Clin. Invest. 112, 1300–1307.

Husain, F.M., Ahmad, I., Al-thubiani, A.S., Abulreesh, H.H., AlHazza, I.M., Aqil, F., 2017. Leaf extracts of *Mangifera indica* L. inhibit quorum sensing- regulated production of virulence factors and biofilm in test bacteria. Front. Microbiol. 8, 727.

Husain, F.M., Ahmad, I., Khan, M.S., Ahmad, E., Tahseen, Q., Khan, M.S., Alshabib, N. A., 2015a. Sub-MICs of Mentha piperita essential oil and menthol inhibits AHL mediated quorum sensing and biofilm of Gram-negative bacteria. Front. Microbiol. 6, 420. https://doi.org/10.3389/fmicb.2015.00420.

Husain, F.M., Ahmad, I., Khan, M.S., Al-Shabib, N.A., 2015b. *Trigonella foenum-graceum* (Seed) extract interferes with quorum sensing regulated traits and biofilm formation in the strains of *Pseudomonas aeruginosa* and *Aeromonas hydrophila*. Evid. Based Complement. Alternat. Med. 2015, 879540.

Husain, F.M., Ahmad, I., 2013. Doxycycline interferes with quorum sensing-mediated virulence factors and biofilm formation in gram-negative bacteria. World J. Microbiol. Biotechnol. 29, 949–957.

Husain, F.M., Ahmad, I., Khan, F.I., Al-Shabib, N.A., et al., 2018. Seed extract of *Psoralea corylifolia* and its constituent Bakuchiol impairs AHL-based quorum sensing and biofilm formation in food-and human-related pathogens. Front. Cell Infect. Microbiol. 8, 351.

Juneja, V.K., Dwivedi, H.P., Yan, X., 2012. Novel natural food antimicrobials. Annu. Rev. Food Sci. T. 3, 381–403.

Kashman, Y., Yosief, T., Carmeli, S., 2001. New triterpenoids from the red sea sponge *Siphonochalina siphonella*. J. Nat. Prod. 64 (2), 175–180.

Kentache, T., Ben Abdelkrim, A., Jouenne, T., Dé, E., Hardouin, J., 2017. Global dynamic proteome study of a pellicle-forming *Acinetobacter baumannii* strain. Mol. Cell Proteo. 16, 100–112.

Le Norcy, T., Niemann, H., Proksch, P., Tait, K., Linossier, I., Réhel, K., Hellio, C., Faÿ, F., 2017. Sponge-inspired dibromohemibastadin prevents and disrupts bacterial biofilms without toxicity. Mar. Drugs. 15, 1–18.

Marti, S., Rodriguez-Bano, J., Catel-Ferreira, M., Jouenne, T., Vila, J., Seifert, H., De, E., 2011. Biofilm formation at the solid-liquid and air-liquid interfaces by *Acinetobacter* species. BMC Res. Notes. 4, 1–4.

Mayer, A.M., Rodríguez, A.D., Berlinck, R.G., Fusetani, N., 2011. Marine pharmacology in 2007–8: Marine compounds with antibacterial, anticoagulant, antifungal, anti-inflammatory, antimalarial, antiprotozoal, antituberculosis, and antiviral activities; affecting the immune and nervous system, and other miscellaneous mechanisms of action. Comp. Biochem. Physiol. C Toxicol. Pharmacol. 153 (2), 191–222.

McClean, K.H., Winson, M.K., Fish, L., Taylor, A., Chhabra, S.R., Camara, M., Daykin, M., Lamb, J.H., Swift, S., Bycroft, B.W., 1997. Quorum sensing and *Chromobacterium violaceum*: exploitation of violacein production and inhibition for the detection of *n*-acylhomoserine lactones. Microbiology 143, 3703–3711.

Morris, A., Masterton, R., 2002. Antibiotic resistance surveillance: action for international studies. J. Antimicrob. Chemother. 49 (1), 7–10.

Müller, W.E., Grebenjuk, V.A., Le Pennec, G., Schröder, H., Brümmer, F., Hentschel, U., Müller, I.M., Breter, H., 2004. Sustainable production of bioactive compounds by sponges—cell culture and gene cluster approach: a review. Mar. Biotechnol. 6 (2), 105–117.

Musthafa, K.S., Sianglum, W., Saising, J., Lethongkam, S., Voravuthikunchai, S.P., 2017. Evaluation of phytochemicals from medicinal plants of Myrtaceae family on virulence factor production by *Pseudomonas aeruginosa*. APMIS 125, 482–490.

O'Toole, G.A., Kolter, R., 1998. Initiation of biofilm formation in *Pseudomonas fluorescens* WCS365 proceeds via multiple, convergent signalling pathways: a genetic analysis. Mol. Microbiol. 28, 449–461.

Pejin, B., Talevski, A., Ciric, A., Glamoclija, J., Nikolic, M., Talevski, T., Sokovic, M., 2014. In vitro evaluation of antimicrobial activity of the freshwater sponge *Ochridaspongia rotunda* (Arndt, 1937). Nat. Prod. Res. 28 (18), 1489–1494.

Rabin, N., Zheng, Y., Opoku-Temeng, C., Du, Y., Bonsu, E., Sintim, H.O., 2015. Agents that inhibit bacterial biofilm formation. Future med. Chem. 7 (5), 647–671.

Raorane, C.J., Lee, J.-H., Kim, Y.-G., Rajasekharan, S.K., García-Contreras, R., Lee, J., 2019. Antibiofilm and antivirulence efficacies of flavonoids and curcumin against *Acinetobacter baumannii*. Front. Microbiol. 10, 990.

Rehman, M.T., Ahmed, S., Khan, A.U., 2016. Interaction of meropenem with 'N' and 'B' isoforms of human serum albumin: a spectroscopic and molecular docking study. J. Biomol. Struct. Dyn. 34, 1849–1864.

Rehman, M.T., AlAjmi, M.F., Hussain, A., Rather, G.M., Khan, M.A., 2019. High-throughput virtual screening, molecular dynamics simulation, and enzyme kinetics identified ZINC84525623 as a potential inhibitor of NDM-1. Int. J. Mol. Sci. 20, 819.

Rehman, M.T., Shamsi, H., Khan, A.U., 2014. Insight into the binding of imipenem to human serum albumin by spectroscopic and computational approaches. Mol. Pharmaceut. 11, 1785–1797.

Russo, T.A., Manohar, A., Beanan, J.M., Olson, R., MacDonald, U., Graham, J., Umland, T.C., 2016. The Response Regulator BfmR Is a Potential Drug Target for Acinetobacter baumannii. mSphere 1(3), pii: e00082-16.

Saad, S., Taher, M., Susanti, D., Qaralleh, H., Awang, A.F., 2012. In vitro antimicrobial activity of mangrove plant *Sonneratia alba*. Asian Pac. J. Trop. Biomed. 2 (6), 427–429.

Sarkar, R., Mondal, C., Bera, R., Chakraborty, S., Barik, R., Roy, P., 2015. Antimicrobial properties of *Kalanchoe blossfeldiana*: a focus on drug resistance with particular reference to quorum sensing-mediated bacterial biofilm formation. J. Pharm. Pharmacol. 67, 951–962.

Shokeen, P., Bala, M., Tandon, V., 2009. Evaluation of the activity of 16 medicinal plants against *Neisseria gonorrhoeae*. Int J Antimicrob Agents. 33 (1), 86–91.

Thanigaivel, S., Vidhya Hindu, S., Vijayakumar, S., Amitava, M., Natarajan, C., John, T., 2015. Differential solvent extraction of two seaweeds and their efficacy in controlling *Aeromonas salmonicida* infection in *Oreochromis mossambicus*: a novel therapeutic approach. Aquaculture 443, 56–64.

Tomaras, A.P., Flagler, M.J., Dorsey, C.W., Gaddy, J.A., Actis, L.A., 2008. Characterization of a two-component regulatory system from *Cinetobacter baumannii* that controls biofilm formation and cellular morphology. Microbiol. Read. Engl. 154, 3398–3409.

Villa, F.A., Gerwick, L., 2010. Marine natural product drug discovery: Leads for treatment of inflammation, cancer, infections, and neurological disorders. Immunopharm. Immunot. 32 (2), 228–323.

Wu, H., Moser, C., Wang, H.Z., Høiby, N., Song, Z.J., 2015. Strategies for combating bacterial biofilm infections. Int. J. Oral Sci. 7 (1), 1–7.